

Supplementary Information

Using $\delta^{13}\text{C}$ of levoglucosan as a chemical clock

I. Gensch^{1,*}, X. F. Sang-Arlt^{1,**}, W. Laumer¹, C. Y. Chan²,
G. Engling^{3,***}, J. Rudolph^{1,4} and A. Kiendler-Scharr¹

¹IEK-8: Troposphere, Forschungszentrum Jülich, Jülich, 52428 Germany

²Institute of Earth Environment, Chinese Academy of Sciences, Xi'an, China

³Department of Biomedical Engineering and Environmental Sciences, National Tsing Hua University, Hsinchu, 30013 Taiwan

⁴Chemistry Department, York University, 4700 Keele Street, Toronto, Ontario, M3J 1P3 Canada

In total, there are seven texts, five figures, five tables, and the document length is fifteen pages.

* Correspondence to I. Gensch, i.gensch@fz-juelich.de

** now at Untersuchungsinstitut Heppeler GmbH, Lörrach, 79539 Germany

*** now at California Air Resources Board, El Monte, CA, 91731 USA

S1 Sampling Locations

The rural sampling site was in Shixing County (SX), which is mainly a rice production area. The station was located 60 km northeast of its central city, Shaoguan, characterized by a relatively low population density. The sampler at that site was installed on the rooftop of a 10 m building, at the edge of a small village, being surrounded by rice straw and vegetable fields. The suburban site was in Ruyuan County (RY), which is covered mainly by natural and self-sown forests. The station was located 20 km south of Shaoguan. The sampler was installed on the rooftop of a seven-story residential building, surrounded by streets with non-intensive traffic flow. The urban site was in a highly developed region with strong industry and dense population. The station was located inside the Sun Yat-sen University campus of Guangzhou Higher Education Mega Center, downwind of the biomass burning source Shaoguan region of in periods when north/northeast winds prevail. The sampler was installed on the rooftop of a central building (~ 20 m height above the ground).

S2 Stable carbon isotope ratio measurements of levoglucosan in ambient aerosol

Ambient aerosol was analyzed for compound specific isotope ratios ($\delta^{13}\text{C}$) using the following steps: liquid extraction of the filter loadings by methanol (LE), liquid injection and thermal desorption of the organic matrices (TD), two-dimensional chromatographic separation of the individual components (2DGC), furnace combustion to CO_2 and H_2O , and CO_2 isotopologues analysis by isotope ratio mass spectrometry (IRMS).

The liquid extraction was done with 10 ml methanol (99.9%, Merck KGaA, Darmstadt, Germany) under ultrasonic agitation for 10 min, followed by syringe filtration (10 ml syringe, SGE analytical Science, Australia and Ø13 mm punched quartz filters, Black ribbon, Schleicher & Schnell, Dassel, Germany). The procedure was repeated for 3 times to maximize the amount of

extracted anhydrosugars from the filter material. The three extracts were mixed together, the solution (ca. 30 ml) was concentrated to 1 ml by a TurboVap 500 Concentration Evaporator Workstation (John Morris Scientific, Sydney, Australia). The concentrated solution was further reduced to 10 μ l. Subsequently, methanol was added to obtain a levoglucosan concentration of ~ 100 ng μ l⁻¹, based on anhydrosugar concentration measurements, considering the area of the extracted filter cut and the anhydrosugar extraction recovery of ca. 90%. The solution was stored in 1.5 ml screw-cap clear glass vials (IVA, Meerbusch, Germany) in a refrigerator at 4 °C until analysis.

Samples consisting of 1 μ l extract solution and 1 μ l internal standard (containing 100 ng Methyl 3, 6-anhydro- α -d- galactopyranoside in methanol, with a known $\delta^{13}\text{C}$) were manually injected into the cooled injection system (CIS) at -30 °C. The organic mixture was thermo-desorbed by increasing the temperature to 220 °C at a heating rate of 12 °C s⁻¹ and holding it there for 2 min. The separation of the volatilized compounds was performed by ‘heart-cut’-two-dimensional gas chromatography. Compared to the method developed for levoglucosan isotope ratio measurements in source filters with rich loadings², the polarity of the used columns was increased. Additionally, smaller diameter and film thickness were chosen to increase the chromatographic performance for small amounts of anhydrosugars in the ambient samples. A custom designed multi-column switching system², including a four-way and a six-way valve as well as a Cooling Trapping System (CTS), allowed selecting and trapping the elute of the first column (Rtx 1301, 30 m length, 0.25 mm ID, 0.5 μ m film thickness, Restek, Bellefonte, USA) in the ‘heart-cut’ time window (19-25 min), containing the internal standard, Methyl 3, 6-anhydro- α -d- galactopyranoside, and the three anhydrosugars of interest (levoglucosan, mannosan, galactosan). The trapped heart-cut fraction in the CTS at -100 °C was transferred to the second polar column (FS-OV 225, 30 m length, 0.25 mm ID, 0.2 μ m film thickness, CS -

Chromatographie Service GmbH, Germany) by abruptly increasing the temperature to 200 °C. Helium was used as carrier gas with a flow of 2 ml min⁻¹. The GC oven temperature program started at 80 °C, was held there for 5 min and increased to 200 °C by 10 °C min⁻¹. Before heating the CTS, the oven temperature was decreased to 80 °C. After heating the CTS, a new temperature program was started raising the GC-oven temperature at a rate of 5 °C min⁻¹ to 200 °C and keeping it there for 16 min. Thus, a baseline separation for the compounds of interest was achieved. The column effluent was split between a quadrupole mass spectrometer (MSD) and an IRMS for detection with a split ratio of 1:3.

After complete oxidation of the individual organic species in the combustion furnace of the GC-IRMS interface at 1030 °C and water removal by a Nafion membrane, CO₂ was analyzed by IRMS (Delta-V Advantage, Thermo Electron GmbH., Bremen, Germany). The m/z 44, 45 and 46 were measured and the isotope ratio $\delta^{13}\text{C}$ derived by using a working reference CO₂, calibrated relative to the V-PDB (Vienna Pee Dee Belemnite) standard. Corrections for ¹⁷O interferences were done as described by¹.

Standard test mixtures of levoglucosan/mannosan/galactosan in methanol were prepared with concentrations of 10, 25, 50 and 100 ng µg⁻¹. A number of isotopic measurements were carried out to improve and evaluate the reproducibility and accuracy of the method. The observed peak areas demonstrate a high precision of the concentration measurements (with a R² of 0.997, 0.996 and 0.981 for levoglucosan, mannosan and galactosan, respectively) (Figure S1). Figure S2 shows that the IRMS delivers good $\delta^{13}\text{C}$ measurement linearity in the range of 50 to 1500 mV. The reproducibility is validated by the good agreement between bulk (EA-IRMS) and compound specific (GC-IRMS) isotopic ratios of all tested species².

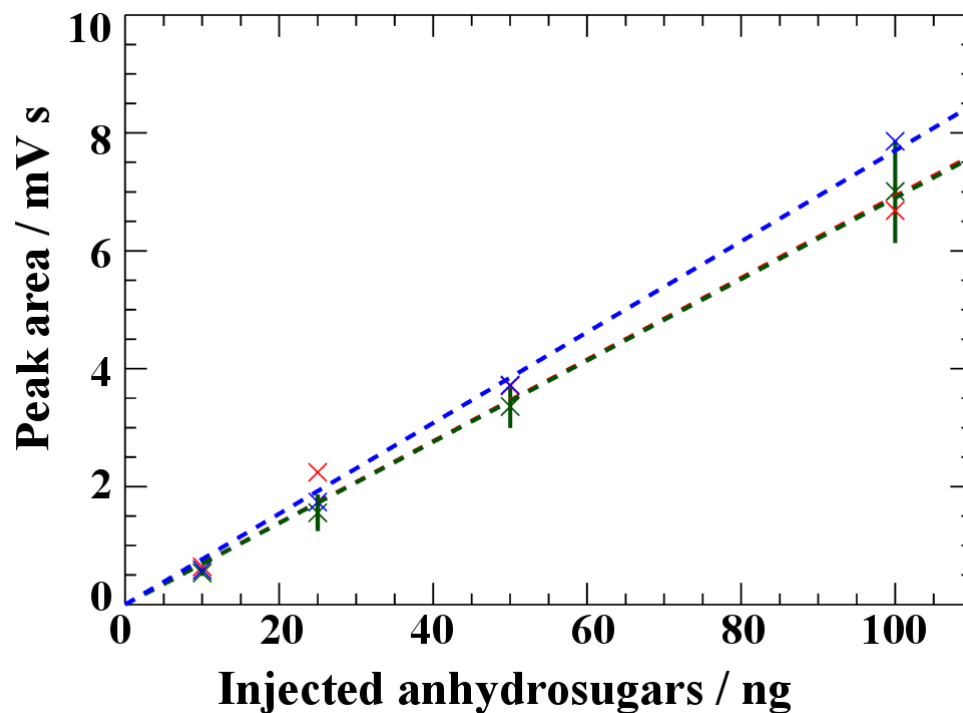


Figure S1: Precision tests for the developed method. The crosses show the peak areas measured by IRMS as function of the injected mass of levoglucosan (green), mannosan (blue) and galactosan (red). The dashed lines are obtained by linear regression analysis of the experimental data, showing r squared of ~ 0.99 .

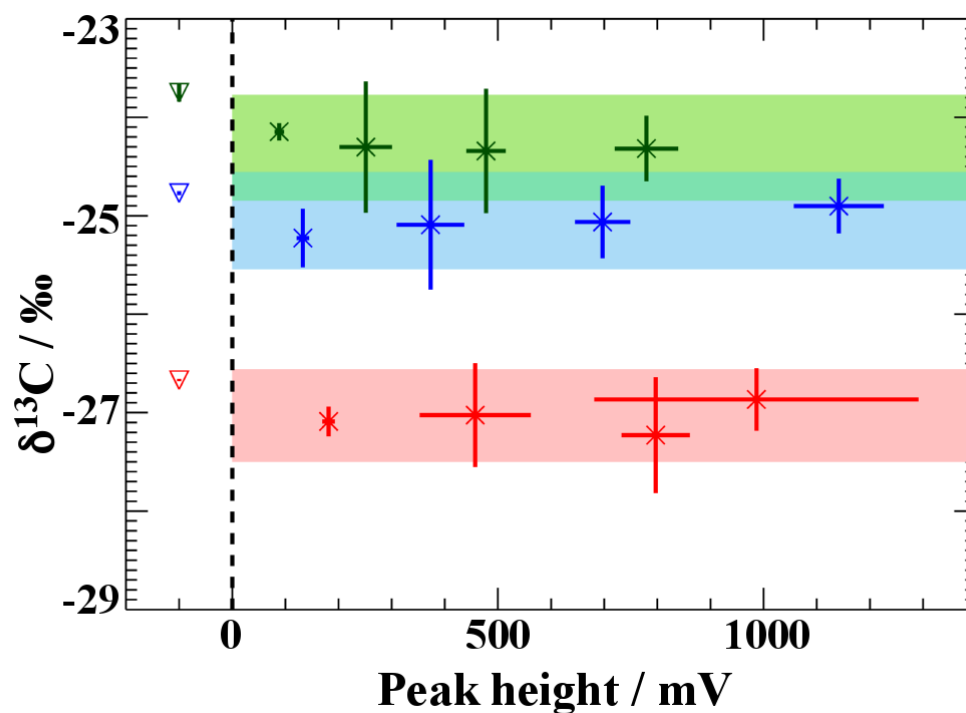


Figure S2: Reproducibility tests for the developed method. The crosses show mean $\delta^{13}\text{C}$ vs. IRMS peak heights (with corresponding standard deviations) for different injected masses of levoglucosan (green), mannosan (blue) and galactosan (red). The triangles represent the bulk $\delta^{13}\text{C}$ values measured by EA-IRMS (¹). The margins of shaded areas are the overall mean $\delta^{13}\text{C}$ \pm overall standard deviation for all test compound specific measurements.

S3 ABL and trajectory heights

The parametrizations used in FLEXPART to determine the mixed layer heights (h_{mix}) are described in detail by Stohl et al.^{3, 4}. Briefly, based on wind and virtual potential temperature fields, as well as on the friction velocity, deduced from surface sensible heat fluxes and decomposed surface stresses, the Richardson number is calculated at each model step. All mentioned parameters are available from ECMWF forecasts. FLEXPART defines h_{mix} as the first model level, for which the Richardson number exceeds a critical value of 0.25. To account for spatial and temporal variations of mixed layer heights on scales which are not resolved by the ECMWF, the convective velocity is also computed from the temperature excess of rising thermals. By using an iterative approach, h_{mix} can be deduced to a desired resolution. An additional, arbitrary parametrization is done to consider variations induced by topography.

FLEXPART provides for every output step the positions of all particles released back in time at the sampling point. Using a cluster analysis, the model congregates all these points in a single one, the 'plume centroid'. Thus, the written out information is as compact as that for a classical 'trajectory', yet accounting for turbulence and convection. For each output time, the latitude, longitude, the height of the plume centroid, as well as the geographically corresponding mixed layer height are delivered. This explains the different 'trajectory' and ABL heights for the 24 hourly generated releases (Figure 2 in the main manuscript), corresponding to one sample.

A proper quantification of the uncertainties introduced with the parameters from the model equations (including the ECMWF data), or with the employed parametrizations to determine the mixed layer and trajectory heights has not yet been done. In one of the few studies on that, Angevine et al.⁵ reviewed the sensitivity of estimates of tracer mixing ratios to different meteorological configurations showing spreads of up to 60% due solely to uncertainties in ABL height and wind speed data.

S4 Implementation of the chemical reaction vs. mixing process contribution in the t_{av} calculations

To determine the likely average duration of the chemical degradation (t_{av}) of levoglucosan during atmospheric transport, back trajectory calculations were performed for each aerosol sample. The isotopic-hydrocarbon-clock (see Eq. 3 in the main manuscript) concept combined with the implementation of fresh BB emission injection as well as their dispersion at different time steps in the trajectory calculations are used to account for the combined effects of chemical aging, fresh aerosol entrainment and dilution on the observed $\delta^{13}\text{C}$ values.

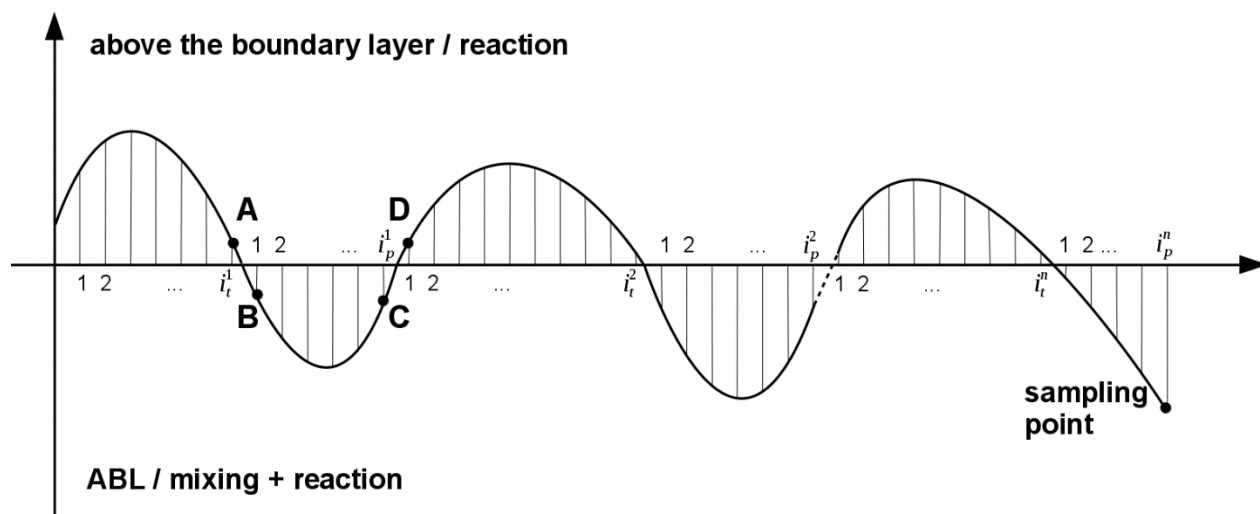


Figure S3: Schematic of the ABL/above-mixed-layer episodes experienced by the investigated air samples. Each episode is divided in 1h-iteration-steps (for details on i_t^n and i_p^n see text).

Conceptually, this approach assumes that $\delta^{13}\text{C}$ of levoglucosan emissions depends on the BB source type at the emission sites. A limitation here is that for any given trajectory, only one average $\delta^{13}\text{C}_0$ value can be used for the BB emissions, thus neglecting the possibility that a given air mass may be influenced by levoglucosan emissions with different isotope ratios. Here we used the isotope ratio for the dominant vegetation type along the trajectory. Each time the air mass trajectory is passing through the mixed layer, an entrainment of fresh BB aerosol (with a

defined $\delta^{13}\text{C}_0$) is assumed. This assumption can be justified by the ongoing fire activities imaged by TERRA/AQUA- MODIS for the considered sampling period and latitudes (see Section S5). During daytime, levoglucosan is chemically degraded by reaction with the OH-radical, resulting in an increase in $\delta^{13}\text{C}$ due to the KIE of this reaction. The addition of fresh BB aerosol to the preexisting one, having an assigned t_{av} , will lead to a decrease of the mean $\delta^{13}\text{C}$ of the levoglucosan present in the probed air mass in its entirety (transfer from A to B in Figure S3). Thus the mean average photochemical age of the aerosol will decrease in the air mass, whenever fresh emissions are added. The extent, to which the entrainment of fresh BB aerosol to a preexisting photochemically aged BB aerosol decreases the $\delta^{13}\text{C}$, depends on the concentration ratio between newly-added and aged levoglucosan. This translates in the calculations in a reduced t_{av} by a reduction factor X_{red} , with $0 \leq X_{red} \leq 1$.

$$t_{av, \text{ chem+mix}} = t_{av, \text{ chem}} \cdot X_{red} \quad (\text{S1})$$

where $t_{av, \text{ chem+mix}}$ is the calculated t_{av} when episodes of aerosol mixing in the ABL alternate with transport above the mixed layer and $t_{av, \text{ chem}}$ is the total daylight time, in case that only chemical degradation takes place.

To quantify the t_{av} reduction, the trajectories are first divided in alternating periods of pure reaction in the free troposphere (index t) and reaction + mixing in the ABL (index p), based on the retro plume calculations RPC vs. ABL heights (Figure S3). Correspondingly, the time spent by the air parcels in each layer along the trajectory is described as following: i_t^1 , i_p^1 , i_t^2 , i_p^2 , ..., i_t^N , i_p^N , from the trajectory origin to the sampling site. This is necessary since at each passage the calculated output concentration and $\delta^{13}\text{C}$ values are taken over as input data for the next layer (see the transition A to B from the layer above ABL into ABL, or C to D, when the air parcel leaves the ABL and passes to the free troposphere). The time is discretized to calculate the concentration reduction during chemical degradation according to the linear one-step methods for

ordinary differential equations approximate solutions. For the FLEXPART output temporal resolution of 1 h, the pseudo first order reaction kinetic of levoglucosan oxidation by OH is described by:

$$\frac{c_0 - c_{1,t}^r}{c_{1,t}^r} = K \quad (\text{S2})$$

where c_0 is the initial concentration, $c_{1,t}^r$ is the concentration after 1 h, the indices r staying for reaction and K is the product of the rate constant and the oxidant mean concentration, i.e. $K = k_{OH} \cdot [OH]_{av}$. Correspondingly, after the first time step the levoglucosan concentration is given as:

$$c_{1,t}^r = \frac{c_0}{1+K} \quad (\text{S3})$$

The derived levoglucosan concentration, at the point where the investigated air parcel enters for the first time the ABL after i_t^1 hours of reaction (A in Figure S3), is:

$$c_{i_t^1}^r = \frac{c_0}{(1+K)^{i_t^1}} \quad (\text{S4})$$

The isotopic fractionation above the mixed layer is described by the isotopic hydrocarbon clock equation (Eq. 3 in the main manuscript).

To calculate the levoglucosan concentration changes in the mixed layer the following assumption is made. The fresh emission is injected into the defined trajectory parcel, occupying a very small fraction ($f = \frac{V_{emis}}{V_{traj}} \ll 1$) in the well mixed trajectory volume. Accordingly, the following applies:

$$c_{1,p}^m = f \cdot c_0 + (1 - f) \cdot \frac{c_0}{(1+K)^{i_t^1}} = \frac{c_0}{(1+K)^{i_t^1}} \cdot [f \cdot (1 + K) + (1 - f)] \quad (\text{S5})$$

In the same time, levoglucosan is degraded by OH. Its concentration after 1 h can be calculated considering reaction:

$$c_{1,p}^{m,r} = \frac{c_0}{(1+K)^{i_t^1+1}} \cdot [f \cdot (1 + K) + (1 - f)] \quad (\text{S6})$$

After i_p^1 hours of both mixing and reaction (point C in Figure S3), when the air parcel leaves the ABL to experience the next above-mixed-layer episode, the concentration can be described as follows:

$$c_{1,p}^{m,r} = \frac{c_0}{(1+K)^{i_t^1+i_p^1}} \cdot \left[f \cdot (1+K)^{i_t^1} \cdot \sum_{k=0}^{i_p^1-1} (1-f)^k + (1-f)^{i_p^1} \right] \quad (S7)$$

As regarding the $\delta^{13}\text{C}$ in the first mixing step, a simple dependence can be derived, based on the fact that the levoglucosan concentration of the new entrainment is much higher compared to the trajectory air. In contrast, its contribution to the total volume is only small⁶.

$$\delta^{13}C_{1,p}^m = \delta^{13}C_0 + \frac{(\delta^{13}C_{i_t^1}^r - \delta^{13}C_0) \cdot c_{i_t^1}^r}{c_{1,p}^m} \quad (S8)$$

According to the Equations S5 and S8, at the point B in Figure S3, when freshly emitted levoglucosan is added, the concentration increases, whereas the $\delta^{13}\text{C}$ value is reduced (see also text above). At the transition from C to D in Figure S3, the opposite occurs; the concentration is reduced through chemical degradation and the $\delta^{13}\text{C}$ value increases due to the KIE.

When applying this approach for the whole trajectory, the concentration at the sampling point can be described as:

$$c_{N,p}^{m,r} = \frac{c_0 \cdot F}{(1+K)^{(\sum_1^N i_t + \sum_1^N i_p)}} \quad (S9)$$

$$\text{where } F = \left[\begin{aligned} & f \cdot (1+K)^{\sum_1^N i_t} \cdot \sum_{k=0}^{i_p^N-1} (1-f)^k + \\ & + f \cdot (1+K)^{\sum_1^{N-1} i_t} \cdot \sum_{k=i_p^N}^{i_p^N+i_p^{N-1}-1} (1-f)^k + \\ & + f \cdot (1+K)^{\sum_1^{N-2} i_t} \cdot \sum_{k=i_p^N+i_p^{N-1}}^{i_p^N+i_p^{N-1}+i_p^{N-2}-1} (1-f)^k + \\ & + \dots + \\ & + f \cdot (1+K)^{i_t^1} \cdot \sum_{k=i_p^N+i_p^{N-1}+\dots+i_p^2}^{i_p^N+i_p^{N-1}+\dots+i_p^1-1} (1-f)^k + \\ & + (1-f)^{\sum_1^N i_p} \end{aligned} \right] \quad (S10)$$

The chemical decay during the 'reduced' t_{av} , along the entire trajectory can be expressed as:

$$c_{N,p}^r = \frac{c_0}{(1+K)^{(\sum_1^N i_t + X_{red} \sum_1^N i_p)}} \quad (S11)$$

X_{red} is deduced by combining Equations S9 and S11:

$$X_{red} = 1 - \frac{\ln(F)}{\sum_1^N i_p \cdot \ln(1+K)} \quad (S12)$$

In this study, t_{av} was calculated for each sample and 24 three-day back trajectories based on the concepts described above. First, a discretization of the mixing and chemical degradation episodes was computed, by using an IDL (Interactive Data Language) program⁷. It has to be noted that chemical reaction was considered only for day-light hours, whereas the mixing calculations were applied also in the night. All equations describing the levoglucosan processing along each trajectory (i.e. Eq. 3 and S1 - S12) were implemented into the developed code. To define K , laboratory kinetic data on the chemical degradation of levoglucosan⁸ were employed. The unknown mixing fraction, f , needed to be specified. Therefore, t_{av} calculations were carried out repeatedly, each time using another value, $f = 0.01, 0.02, 0.09, 0.1, 0.2, \dots, 0.9$. As described in the main manuscript, the data points were divided into two sets depending on the dominant typical vegetation along the trajectory.. For each set of $\delta^{13}\text{C}$ vs. the derived t_{av} , a regression analysis was separately done, on the assumption of linear dependence between t_{av} and $\delta^{13}\text{C}$, which is predicted by the isotope ratio clock equation (Eq. 3 in the main manuscript). For both data sets of investigated BB source types, the best linear correlation between the measured levoglucosan $\delta^{13}\text{C}$ and the extent of its chemical processing (translated into the calculated t_{av}) was reached for $f = 0.1$, yielding Pearson ρ values of 0.56 and 0.57, respectively. Both coefficients are consistent within the 90% confidence intervals. Therefore a mixing fraction of 0.1 was chosen to be implemented in the Equation S10 to describe the entrainment of fresh BB aerosol in each simulated trajectory mixing volume. Accordingly, the resulting values for t_{av} were used in the analyses presented in Section 5, main manuscript.

S5 FLEXPART three-day back trajectories of the sampled aerosol

Figure S4 summarizes all three-day back trajectories of the studied aerosol at the rural, suburban and urban sampling sites, showing that a significant contribution of C4 plant combustion to the primary emissions can be ruled out. The sampling period was characterized by strong fire activities (<https://firms.modaps.eosdis.nasa.gov/map/#z:5.0;c:110.230,27.663>).

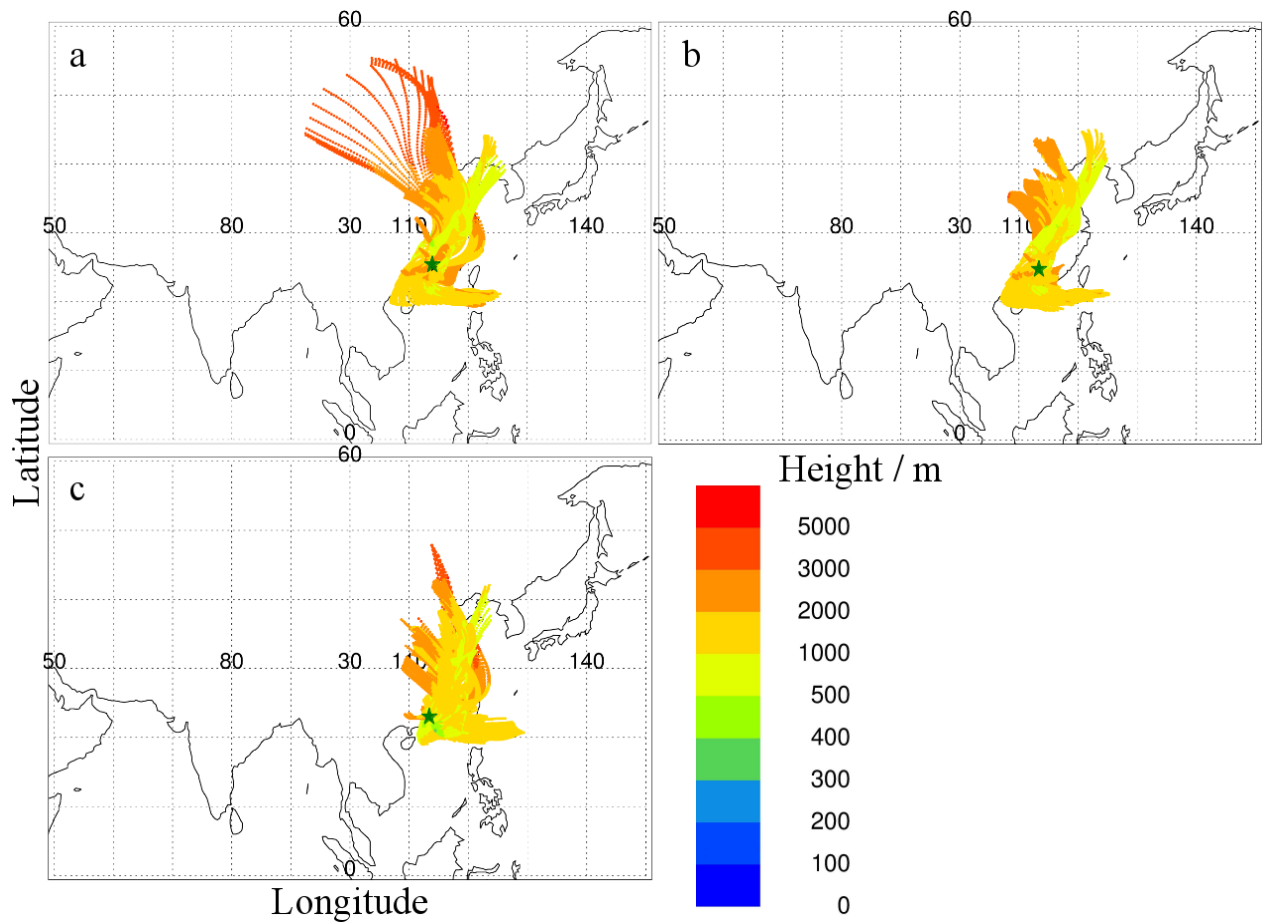


Figure S4: Summary of all three-day back trajectories of the studied aerosol at the rural (a), suburban (b) and urban (c) sampling sites. 24 hourly RPC positions and the corresponding heights in the shown color code are depicted for the last three days before sampling. The green stars represent the position of the sampling site.

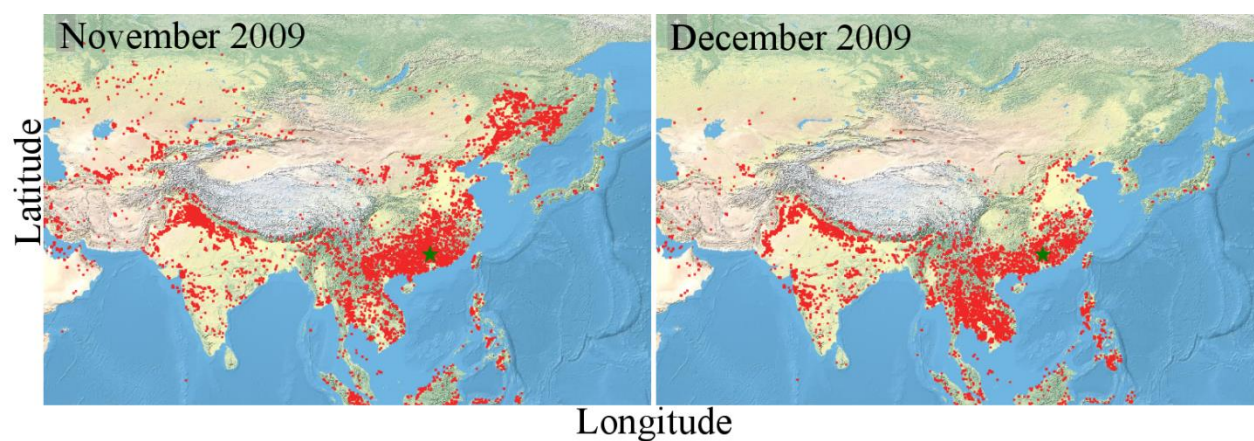


Figure S5: Cumulative active fire detections provided by the NASA FIRMS (Fire Information for Resource Management System) for the investigated area during November (left panel) and December (right panel) 2009.

S6 Correlation between the concentrations of levoglucosan and total carbon

Table S1: Linear correlation coefficients for the dependence between the concentrations of levoglucosan and TC in aerosols at three locations (details for sampling sites see S1).

Sampling Location	Pearson Correlation Coefficient	R^2	N^a	Concentration Range ^b
Rural	0.98	0.96	24	7.2, 18.2, 31.1
Suburban	0.92	0.84	22	5.7, 15.0, 29.4
Urban	0.98	0.96	27	7.0, 16.6, 41.9

^a Number of samples where both levoglucosan and TC could be measured

^b Given are the 10-percentile, median and 90-percentile of the TC concentration in $\mu\text{g m}^{-3}$.

S7 Statistical evaluation and comparison of t_{av} calculated by the Flexpart simulations and those derived from the measured levoglucosan carbon isotope ratios

Table S2: Regression data for linear least square fits in Figure 3 (main manuscript).

	CAT1	CAT2
Pearson Correlation Coefficient	0.518	0.522
R^2	0.268	0.258
Intercept	$-23.1 \pm 0.2 \text{ ‰}$	$-24.9 \pm 0.2 \text{ ‰}$
Slope	$0.072 \pm 0.024 \text{ ‰ h}^{-1}$	$0.076 \pm 0.021 \text{ ‰ h}^{-1}$
Number of data points	26	37

Table S3: Basic statistics for $t_{av, traj}$

Source type	Average	Standard deviation	N	Error of mean	Range ^a
CAT1	9.1 h	4.5 h	26	0.9 h	2.6, 9.7, 14.6
CAT2	12.6 h	5.0 h	37	0.8 h	5.7, 15.0, 29.4
All	11.1 h	5.0 h	63	0.6 h	4.7, 11.1, 17.5

^a Given are the 10-percentile, median and 90-percentile of t_{av} in h.

Table S4: Basic statistics for $t_{av, \delta}$

Source type	Average	Standard deviation	N	Error of mean	Range ^a
CAT1	6.1 h	9.4 h	26	1.9 h	-3.9, 6.3, 19.4
CAT2	17.1 h	10.4 h	37	1.8 h	2.7, 16.0, 30.4
All	12.1 h	11.5 h	63	1.5 h	-1.3, 11.3, 27.9

^a Given are the 10-percentile, median and 90-percentile of t_{av} in h.

Table S5: Basic statistics for the difference between $t_{av, \delta}$ and $t_{av, traj}$

Source type	Average	Standard deviation	N	Error of mean	Range ^a
CAT1	3.0 h	8.0 h	26	1.6 h	-14.5, -1.9, 7.1
CAT2	4.5 h	8.9 h	37	1.5 h	-9.1, 5.3, 15.2
All	1.1 h	9.5 h	63	1.2 h	-11.1, 1.4, 14.1

^a Given are the 10-percentile, median and 90-percentile of t_{av} in h.

We acknowledge the use of data and imagery from LANCE FIRMS operated by the NASA/GSFC/Earth Science Data and Information System (ESDIS) with funding provided by NASA/HQ. Specifically we acknowledge the use of the MODIS Collection 6 NRT Hotspot / Active Fire Detections MCD14DL data (available on-line [<https://earthdata.nasa.gov/firms>], DOI: 10.5067/FIRMS/MODIS/MCD14DL.NRT.006).

1. Brand, W. A.; Assonov, S. S.; Coplen, T. B., Correction for the ^{17}O interference in $\delta(^{13}\text{C})$ measurements when analyzing CO_2 with stable isotope mass spectrometry (IUPAC Technical Report). *Pure Appl. Chem.* **2010**, 82, 1719-1733.
2. Sang, X. F.; Gensch, I.; Laumer, W.; Kammer, B.; Chan, C. Y.; Engling, G.; Wahner, A.; Wissel, H.; Kiendler-Scharr, A., Stable Carbon Isotope Ratio Analysis of Anhydrosugars in Biomass Burning Aerosol Particles from Source Samples. *Environ. Sci. Technol.* **2012**, 46, 3312-3318.
3. Stohl, A.; Forster, C.; Frank, A.; Seibert, P.; Wotawa, G., Technical note: The Lagrangian particle dispersion model FLEXPART version 6.2. *Atmos. Chem. Phys.* **2005**, 5, 2461-2474.
4. Stohl, A.; Sodemann, H.; Eckhardt, S.; Frank, A.; Seibert, P.; Wotawa, G., The Lagrangian particle dispersion model FLEXPART version 8.2. In <https://www.flexpart.eu/>, 2010.
5. Angevine, W. M.; Brioude, J.; McKeen, S.; Holloway, J. S., Uncertainty in Lagrangian pollutant transport simulations due to meteorological uncertainty from a mesoscale WRF ensemble. *Geosci. Model Dev.* **2014**, 7, 2817-2829.
6. Rudolph, J., *Gas Chromatography-Isotope Ratio Mass Spectrometry*. Blackwell Publishing: 2007.
7. Bauer, R., *IDL Referenz der ICG-Daten-Struktur*. Forschungszentrums Jülich: Jülich, 2006.
8. Sang, X. F.; Gensch, I.; Kammer, B.; Khan, A.; Kleist, E.; Laumer, W.; Schlag, P.; Schmitt, S. H.; Wildt, J.; Zhao, R.; Mungall, E. L.; Abbatt, J. P. D.; Kiendler-Scharr, A., Chemical stability of levoglucosan: An isotopic perspective. *Geophys. Res. Lett.* **2016**, 43, 5419-5424.